Conducting and magnetic hybrid polyaniline/nickel composites

Conducting and magnetic hybrid polyaniline/nickel composites

Marek Jurča[a], Jarmila Vilčáková[a], Natalia E. Kazantseva[a], Jan Prokeš[b], Miroslava Trchová[c], Jaroslav Stejskal[a,c,*]

[a]*University Institute, Tomas Bata University in Zlin, 760 01 Zlin, Czech Republic*
[b]*Charles University, Faculty of Mathematics and Physics, 180 00 Prague 8, Czech Republic*
[c]*University of Chemistry and Technology, Prague, 166 28 Prague 6, Czech Republic*

AUTHOR INFORMATION

Corresponding Author

Jaroslav Stejskal – *University Institute, Tomas Bata University in Zlin, 760 01 Zlin, Czech Republic; University of Chemistry and Technology, Prague, 166 28 Prague 6, Czech Republic;* orcid.org/0000-0001-9350-9647; Email: stejskal@utb.cz

Authors

Marek Jurča – *University Institute, Tomas Bata University in Zlin, 760 01 Zlin, Czech Republic;* orcid.org/0000-0001-5917-4468

Jarmila Vilčáková – *University Institute, Tomas Bata University in Zlin, 760 01 Zlin, Czech Republic;* orcid.org/0000-0002-1216-2862

Natalia Kazantseva – *University Institute, Tomas Bata University in Zlin, 760 01 Zlin, Czech Republic;* orcid.org/0000-0003-4884-5371

Jan Prokeš – *Charles University, Faculty of Mathematics and Physics, 180 00 Prague 8, Czech Republic;* orcid.org/0000-0002-8635-7056

Miroslava Trchová – *University of Chemistry and Technology, Prague, 166 28 Prague 6, Czech Republic;* orcid.org/0000-0001-6105-7578

ABSTRACT

Hybrid organic/inorganic polyaniline/nickel composites were prepared by the in-situ oxidation of aniline hydrochloride with ammonium peroxydisulfate in the presence of various portions of nickel microparticles. Electron microscopies demonstrated the coating of nickel with polyaniline. FTIR and Raman spectroscopies indicated the reduced degree of polyaniline protonation. As a consequence, the composites containing 7.2–58.8 wt% of nickel had the

conductivity of the order of 10^{-3}–10^{-2} S cm^{-1}, i.e. several order of magnitude lower than the conductivity of polyaniline or nickel. The conductivity as a function of applied pressure is also reported. Relatively low conductivity of composites is explained by the partial reduction of polyaniline with hydrogen gas evolved during the synthesis and consequent hydrogenation of polyaniline catalysed by nickel. The accompanying partial dissolution of nickel manifests itself by the reduced composite yield. The reason why hydrogen is generated mainly after the synthesis of polyaniline is discussed. The magnetic properties afforded by nickel are also reported. The composites dispersed in thermoplastic polyurethane matrix providing mechanical properties have been tested for electromagnetic interference shielding.

Keywords: Conducting polymer, polyaniline, nickel, hybrid conducting/magnetic composites, electromagnetic interference shielding.

1. Introduction

Hybrid organic/inorganic conducting and magnetic materials are of interest both from the academic point of view and for application in various directions. Special attention has been paid to the organic component that was represented by a conducting polymer, such as polyaniline [1], which also served to improve the composite processing. The inorganic part may display both the electrical and magnetic properties. Nickel [2, 3], iron [4] or various iron oxides [5] and ferrites [6] are examples. Electromagnetic interference shielding is probably the most widely studied field where both the conductivity and magnetic properties play important role [2, 7–9].

If we limit ourselves to polyaniline/nickel systems, hybrid electrode materials [10– 13] should be mentioned in this context as applications relying on electrical or electrochemical properties. The electrocatalysis of hydrogen evolution reaction [14] or the use in supercapacitor electrodes [15] are additional examples. Magnetic properties of nickel in the composites have also been exploited. Hybrid adsorbents of environmental pollutants, viz. organic dyes of heavy-metal ions [10, 16] or photocatalysts of dye decomposition have been reported in the literature [17–23]. Such composites are conveniently separable by the application of magnetic field. Similarly in magnetorheology the viscosity of suspensions is controlled by external magnetic field [4].

The polyaniline/nickel hybrids of above type have been prepared by the electrochemical deposition of nickel on polyaniline [14] or reduction of nickel(II) ions with ethylene glycol [23, 24]. A reverse strategy is illustrated by the in-situ coating of nickel foam with polyaniline [9]

or electropolymerization of aniline at such macroporous substrate [15]. The similar deposition of polyaniline on nickel-coated carbon fibres also belongs to this category of preparations [7]. Finally, polyaniline and nickel particles can be simply mixed together with some additives [6, 13, 25]. The present study also combines an organic conducting polymer, polyaniline, with inorganic component, nickel metal. In-situ deposition of conducting polyaniline shell on nickel particles, i.e. the coating of nickel immersed in the reaction mixture used for the oxidation of aniline to polyaniline, has not yet been studied in detail. This is probably due to a priori doubt if nickel can withstand the strongly acidic and oxidizing aqueous medium typical of polyaniline preparation. Nevertheless, the in-situ polymerization of aniline was reported to deposit polyaniline on 10–50 nm nickel nanoparticles functionalized with 4-aminobenzoic acid [2]. The composite was tested for microwave absorption, but neither its conductivity nor magnetic properties have been provided. Polyaniline was also prepared in the suspension of cellulose and nickel nanoparticles [21] and the composite was used as a photocatalyst in the Reactive Orange 16 dye removal but, again, without reporting electrical or magnetic properties. The preparation and properties of polyaniline/nickel hybrids are discussed in the present communication.

The present communication is aimed at the preparation of a new functional material and the characterization of its electrical and magnetic properties. Its potential application is illustrated by the electromagnetic interference shielding. Other fields of application, however, are open to discussion and they are represented by organic dye adsorbents separable by magnetic field, photocatalysts for the dye decomposition in environmental issues, electrocatalysts in organic hydrogenation reactions or in hydrogen generation by water splitting.

2. Experimental

2.1. Preparation

Nickel microparticles (99.8 wt% nickel; Goodfellow, Great Britain) with a hedgehog-like morphology were used as a conducting and magnetic substrate with a normal size distribution and mean diameter 5.5 μm. Aniline hydrochloride (2.59 g; Sigma-Aldrich) was dissolved in water to 100 mL, ammonium peroxydisulfate (5.71 g; Lach-Ner, Czech Republic) also to the same volume. Both solutions were mixed at room temperature, specified amount nickel powder was added, and the mixture was gently stirred with a mechanical stirrer. The concentrations of reactants used for the preparation of polyaniline were 0.1 M aniline hydrochloride and 0.125 M ammonium peroxydisulfate. The originally colourless mixture gradually turned blue and finally green as the polymerization of aniline was completed in ca. 30 min. The gentle sparkling was then heard when listened close to the beaker, suggesting the

hydrogen-gas evolution. After 1 h the solids were separated by filtration, rinsed with 1 M hydrochloric acid, followed by copious amounts of ethanol and dried in air.

2.2. Characterization

Scanning electron micrographs were taken with an ultra-high-resolution electron microscope MAIA3 (Tescan, Czech Republic). Transmission electron microscope JEOL JEM 2000 FX (JEOL, Japan) was equipped with energy dispersive X-ray analysis (EDAX) of elemental composition. In addition, weight fraction of nickel in the composites was determined as an ash composed by nickel(II) oxide [26], after the correction for oxygen content.

ATR FTIR spectra of the powdered samples were analysed using Nicolet 6700 spectrometer (Thermo-Nicolet, USA) using a reflective ATR extension GladiATR (PIKE Technologies, USA) with a diamond crystal. Spectra were registered in the 4000–400 cm^{-1} range with a deuterated L-alanine-doped triglycine sulfate detector at 4 cm^{-1} resolution, 64 scans and using Happ-Genzel apodization. The spectra were corrected for the presence of carbon dioxide and humidity in optical path.

Raman spectra were collected with a Thermo Scientific DXR Raman microscope equipped with a 780 nm line laser using 4 mW power. The spot size of the laser was focused by 50× objective. The scattered light was analysed by a spectrograph with holographic gratings (1200 lines per mm), and a 50 μm pinhole width. The acquisition time was 10 s with 10 repetitions.

The conductivity of polyaniline/nickel composites was determined by a four-point van der Pauw method on pellets 10 mm in diameter and *ca* 1 mm thickness compressed at 527 MPa. The dependence of resistivity on applied pressure has also been characterized by van der Pauw method. The powder was placed in a cylindrical glass cell with 10 mm inner diameter between an insulating support and a glass piston carrying four platinum/rhodium electrodes on the perimeter of its base. The experimental set-up included a current source Keithley 220, a Keithley 2010 multimeter and a Keithley 705 scanner with a Keithley 7052 matrix card. The pressure was controlled with a L6E3 load cell (Zemic Europe BV, The Netherlands). The actual thickness of the sample was determined for each pressure using an ABS Digimatic indicator Mitutoyo, model ID-S112X.

Magnetic characteristics of prepared nanocomposites were determined with a vibrating sample magnetometer (VSM, Model 7407, USA) in the intensity of magnetic field range from –10 to +10 kOe.

For the electromagnetic interference shielding, polyaniline/nickel hybrids were mixed with thermoplastic polyurethane (TPU) Estane 58271 TPU (The Lubrizol Corporation, Wickliffe, OH, USA) in a micro compounder (Xplore Instruments BV, Sittard, The Netherlands) with a capacity of 5 cm^3. Prior to mixing, TPU was dried at 90 °C for 15 h. The materials were melt-mixed using 100 rpm speed at 150 °C for 5 minutes to achieve good dispersion of the polyaniline/nickel filler at 60 wt% content. Under such conditions no changes in the molecular structure of polyaniline are expected [27].

Electromagnetic interference shielding parameters of polyaniline/nickel powders dispersed in TPU were recorded with a PNA-L Network Analyzer Agilent N5230A (Agilent Technologies, Santa Clara, CA, USA) by a waveguide method in the frequency range 8–12 GHz (X-band). The sample of 2 mm thickness was cut to fit the sample holder (10×23 mm^2).

3. Results and discussion

3.1.Chemistry of preparation

The preparation outlined above is expected to produce 2.17 g of polyaniline hydrochloride [28]. The theoretical yield in the presence of *G* g nickel thus 2.17+*G* g. In present syntheses, however, this limit has not been reached and true yield *Y* was close to 80 % of the expectation Y_{th} [28]. This may have two reasons: (1) the partial dissolution of nickel, as suspected by the release of hydrogen gas at the final stage of the preparation, and (2) the decrease in polyaniline protonation. This is also in the accordance lower content of nickel in the composites, *w*, compared to the expectation, w_{th} (Table 1).

Table 1. The content of nickel in 200 mL of reaction mixture, *G*, the composite yield, *Y*, compared with theoretical expectation, Y_{th}, the weight fraction of nickel in the composite, *w*, again compared with the theory, w_{th}.

***G*, g**	***Y*, g**	**Y_{th}, %**	***w*, wt%**	**w_{th}, wt%**
0	2.329	107.3	0	0
0.5	2.198	82.3	7.2	18.7
1	2.540	80.1	19.9	31.5
1.5	3.250	88.5	29.4	40.9
2	3.263	78.2	40.2	48.0
3	4.152	80.3	53.7	58.0
4	5.087	82.4	58.8	64.8

The following scenario is offered: The starting reaction mixture contains aniline hydrochloride, ammonium peroxydisulfate (Fig. 1). Hydrochloric acid present in this mixture does not dissolve nickel, even in the presence of peroxydisulfate. As the conversion from aniline to polyaniline proceeds, sulfuric acid is produced as a by-product. This manifests itself by the drop in pH [1]. In the contrast to hydrochloric acid, dilute sulfuric acid dissolves nickel [29]. If nickel is present in the reaction mixture, the generated sulfuric acid reacts with this metal at the simultaneous evolution of hydrogen gas, $Ni + H_2SO_4 \rightarrow H_2(g) + NiSO_4$, as indeed observed in the experiment. Semiquantitative estimate can be made as follows: In present syntheses, 20 mmol (2.59 g) of aniline hydrochloride enters the reaction. According to the assumed stoichiometry (Fig. 1), 25 mmol of sulfuric acid would be available for the dissolution of nickel (25 mmol; 1.47 g). For that reason, the polyaniline/nickel composite contains always less nickel than expected, $w < w_{th}$ (Table 1).

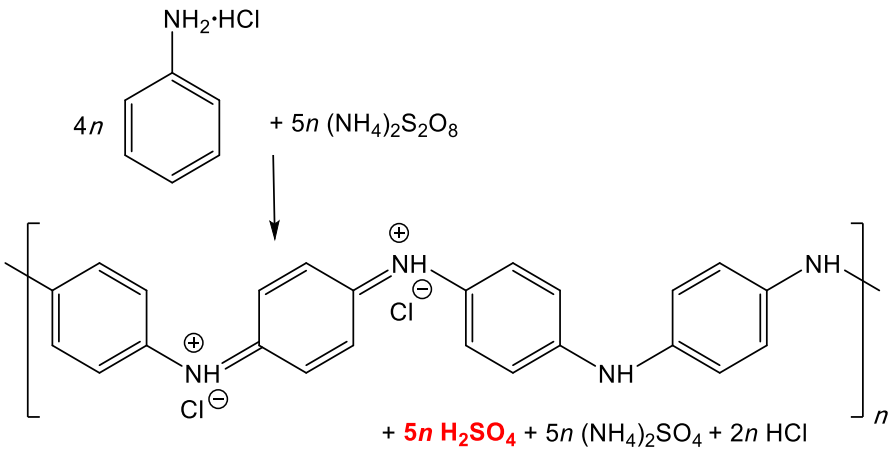

Fig. 1. Aniline hydrochloride is oxidized with ammonium peroxydisulfate to polyaniline salt. Sulfuric acid is one of the by-products. In addition to chloride anions, also hydrogen sulfate ones may also act as counter-ions.

The idealized formula of polyaniline assumes the equal fraction of "oxidized" protonated quinonediimine units, *x*, that are responsible for the polaronic charge-carrier generation and for occurrence of the conductivity, and non-protonated "reduced" benzenoid constitutional units, *y* (Fig. 2), i.e. $x = y$ (Fig. 1). Nickel is currently used as a catalyst in the hydrogenation of organic compounds. For that reason a part of quinonediimine constitutional units in polyaniline may become hydrogenated by in-situ generated hydrogen gas to benzenoid ones, $y > x$. The *number of imine nitrogen sites* available for the protonation will be reduced and, consequently, the conductivity would become lower. In addition, the sulfuric acid is

consumed in the nickel dissolution, the pH of reaction mixture will become less acidic, and the *fraction of protonated nitrogen sites* will decrease, as the salt/base conversion (Fig. 2) will shift in favour of non-conducting polyaniline base. This will further reduce the composite conductivity.

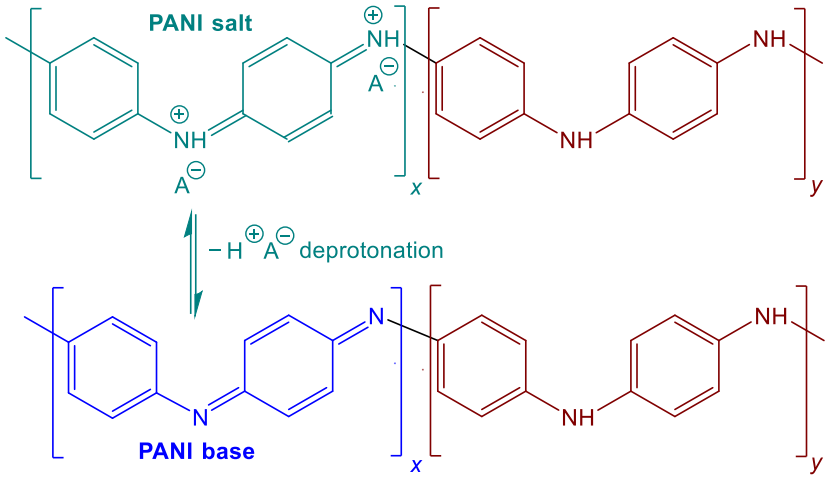

Fig. 2. Polyaniline salt and base. A^- is chloride, sulfate, or hydrogen sulfate counter-ion.

3.2. Morphology

Nickel microparticles had the size of the units of micrometres with irregular hedgehog shape (Fig. 3a). Fig. 3b shows the morphology of polyaniline/nickel (19.9 wt%) composite. It should be kept in mind that the volume fraction of nickel is much lower due to the large difference between nickel and polyaniline densities 8.9 and 1.4 g cm^{-3}, respectively. For that reason, only dominating voluminous globular polyaniline coating is visible on the micrograph. The coating of nickel microparticles with polyaniline is also demonstrated by transmission electron microscopy (Fig. 4). Some free polyaniline accompanies them.

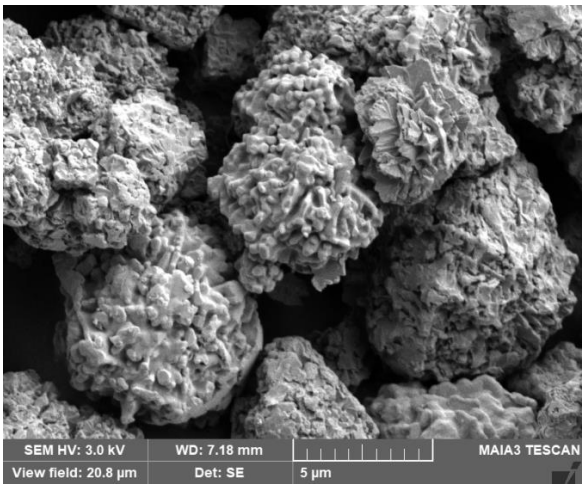

(a) Nickel

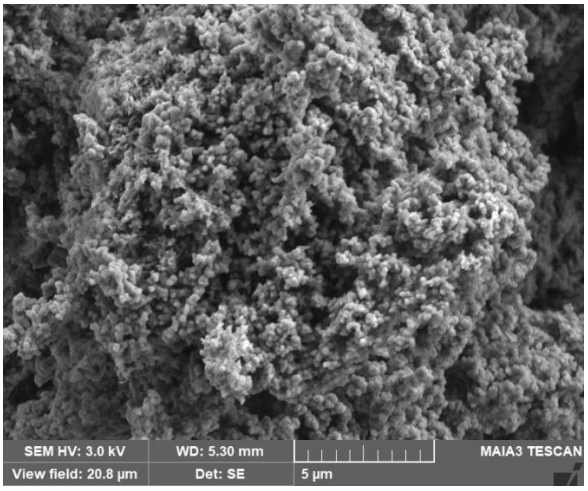

(b) Polyaniline/nickel

Fig. 3. Scanning electron micrograph of nickel microparticles (a) before and (b) after the coating with polyaniline.

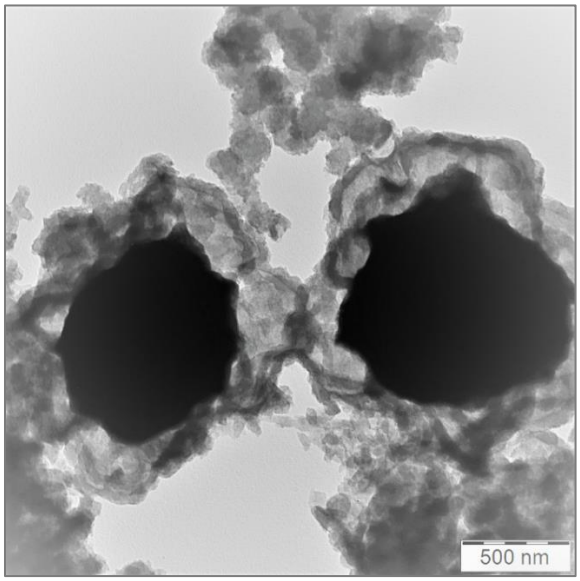

Fig. 4. The transmission electron micrograph of polyaniline/nickel (19.9 wt%) composite.

The presence of nickel is documented by the EDAX performed with two samples where the content of nickel was found as 19.9 and 40.2 wt% (Fig. 5). The fraction of nickel found by EDAX is considerably lower (Table 2). This is understandable because EDAX is the method of surface characterization and the access to the nickel surfaces is restricted by the polyaniline coating as demonstrated by carbon and nitrogen content. Sulfur and oxygen come from hydrogen sulfate counter-ions produced by the reduction of peroxydisulfate oxidant, oxygen additionally from potential *p*-benzoquinone by-products, and chlorine from chloride counter-ions. If we abstain from the marginal content of sulfur, the atomic Cl/N ratio expected from the ideal stoichiometry would be 0.5 (Fig. 2). The EDAX finds this ratio 0.24 and 0.32, i.e. it confirms the reduced number of quinonediimine units that are able to be protonated.

Table 2. EDAX analysis of polyaniline/nickel composites with 19.9 and 40.2 wt% nickel found as an ash.

Element	19.9 wt% Ni	40.2 wt% Ni
C	65.6	65.2
N	11.7	11.7
O	11.9	6.4
S	0.7	0.5
Cl	2.9	3.8
Ni	6.5	11.7
Pt	0.6	0.7

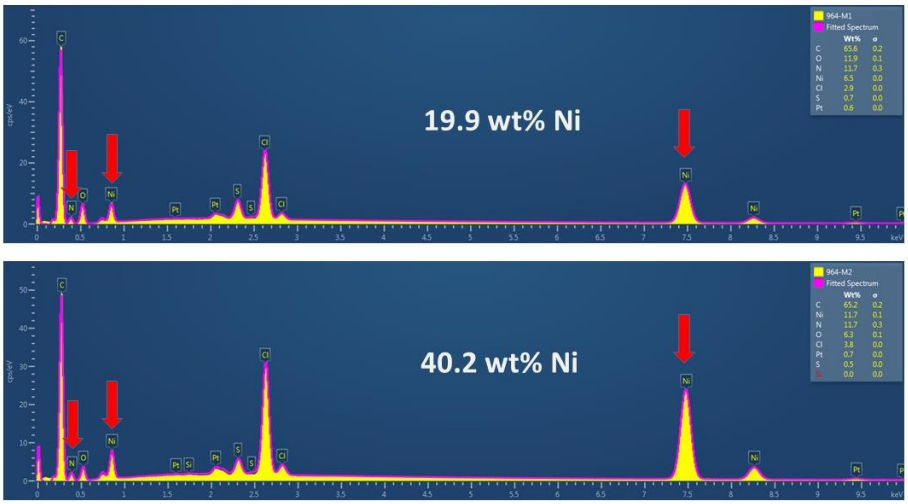

Fig. 5. EDAX analysis of polyaniline/nickel composites containing 19.9 and 40.2 wt% nickel. The peaks corresponding to nickel are marked with an arrow.

3.3. FTIR spectra

ATR FTIR spectra of various amounts of nickel particles coated with polyaniline (Fig. 6) differ from the spectrum of polyaniline salt prepared by the same way (spectrum 0) and from the spectrum of deprotonated polyaniline (spectrum of polyaniline base). Two main bands with maxima situated at 1553 and 1480 cm^{-1}, assigned to the quinonoid and benzenoid ring-stretching vibrations, respectively, are shifted to 1580 and 1493 cm^{-1}, like in the spectrum of deprotonated polyaniline [1]. A small peak observed at 1374 cm^{-1} is also typical of polyaniline base and it is attributed to a C–N stretching vibrations in the neighbourhood of a quinonoid ring. The bands with maxima at 1300 and 1236 cm^{-1} in the spectrum of polyaniline salt belong to π-electron delocalization and to the band of C~$N^{+\bullet}$ stretching vibrations in the polaronic structure, respectively [1]. The former is much higher in comparison to the spectra of nickel particles coated with polyaniline. The contribution of the C–N stretching vibrations of a secondary aromatic amine is expected in the spectrum of polyaniline base [1]. The broad band with maximum situated at 1114 cm^{-1} has been assigned to the vibrations of the –NH^{+}= structure in the spectrum of polyaniline salt. In the spectrum of deprotonated polyaniline, the aromatic C–H in-plane bending modes are usually observed in this region. The band situated at about 800 cm^{-1} belongs to C–H deformations in the *para*-substituted ring [1]. We conclude that the spectra of nickel particles coated with polyaniline exhibit the bands characteristic of polyaniline base with enhanced amount of quinonoid units. The contribution of some bands typical for protonated polyaniline is also evident.

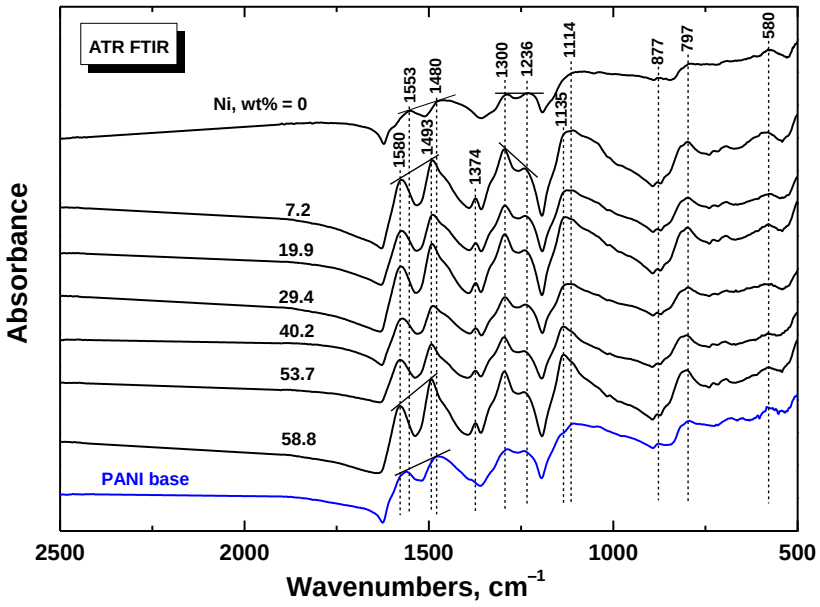

Fig. 6. ATR FTIR spectra polyaniline/nickel composites with various nickel content. Spectrum of deprotonated polyaniline (PANI base) is included for comparison.

3.4. Raman spectroscopy

Raman spectra of various amount of nickel particles coated with polyaniline (Fig. 7) differ from the spectrum polyaniline prepared by the same way or of standard polyaniline salt or (spectrum polyaniline M = 0 and spectrum polyaniline S). The band with maximum at 1602 cm^{-1} connected with C=C stretching vibrations in a quinonoid ring is slightly shifted to 1590 cm^{-1}. This band is situated at 1609 cm^{-1} in the spectrum of polyaniline base (spectrum PANI B). The peak with a maximum at 1514 cm^{-1} of the N–H deformation vibrations associated with the semiquinonoid structures in the spectrum of protonated polyaniline (spectrum PANI S) is missing in the spectrum of polyaniline base and also in the spectra of nickel coated with polyaniline. In contrast, the band with maximum at 1464 cm^{-1} assigned to C=N vibrations in the quinonoid units dominates the spectrum of polyaniline base and also the spectra of nickel particles coated with polyaniline. The peak situated at 1415 cm^{-1} associated with phenazine-like structures appears in the spectra of these samples. The bands with maxima at 1380 and 1332 cm^{-1} of the $C{\sim}N^{+\bullet}$ vibrations of localized and delocalized polaronic structures, respectively, and observed in the spectra of polyaniline salt, are only sporadically detected in nickel particles coated with polyaniline. In the spectrum of polyaniline base, they are practically missing. Benzene-ring deformation vibrations are connected with the band at 1232 cm^{-1} in the spectrum of polyaniline salt and at 1223 cm^{-1} in the spectrum of polyaniline base and nickel particles coated with polyaniline. The band at 1177 cm^{-1} corresponds to the C–H in-plane bending vibrations of semi-quinonoid or benzenoid rings in polyaniline salt and at 1162 cm^{-1} in the spectrum of polyaniline base and of polyaniline/nickel composites. In the spectrum of polyaniline salt we observe the band at 812 cm^{-1} linked to the benzene-ring deformations, at 577 cm^{-1} assigned to the in-plane amine deformation vibrations of the polyaniline salt and out-of-plane deformations of the ring at 520 and 423 cm^{-1}. In contrast to this shape, a broad structural band with local maxima at 851, 780 and 747 cm^{-1} of benzene-ring deformations of variously substituted aromatic rings is observed in the spectrum of polyaniline base and of nickel particles coated with polyaniline. This band also includes phenazine-like structures. We thus conclude that all spectra of nickel particles coated with polyaniline are very close to the spectrum of polyaniline base and only sporadically contain the features corresponding to the spectrum of polyaniline salt.

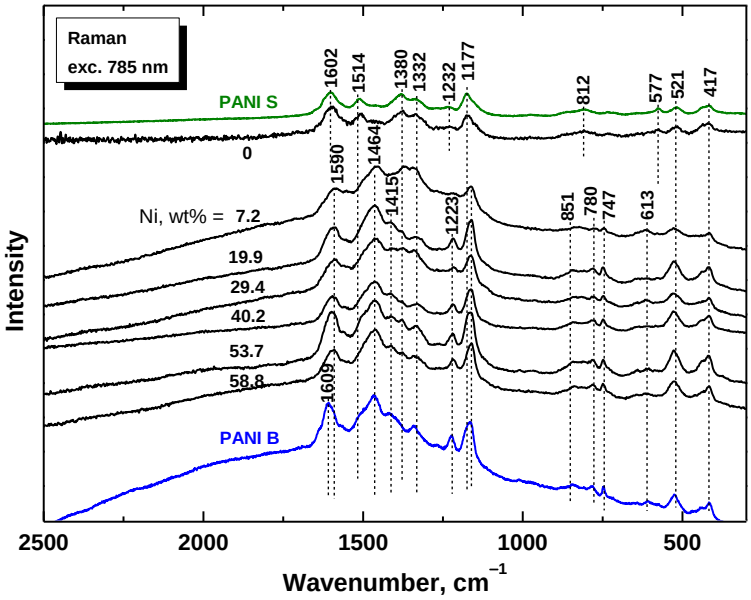

Fig. 7. Raman spectra of polyaniline/nickel composites with various nickel content. Spectra of standard polyaniline (PANI S) and deprotonated polyaniline (PANI base) are included for comparison.

3.5. Conductivity

The conductivity of polyaniline/nickel composites is in all cases lower than the conductivity of individual components, polyaniline and nickel (Table 3), but still at the level, which is satisfactory for various applications based on electrical properties. The spectroscopic analysis and EDAX suggest that this is due to the reduced degree of protonation of polyaniline as discussed above.

Table 3. Electrical and magnetic properties of polyaniline/nickel composites with various nickel content, *w*: Conductivity, σ, saturation magnetization, M_s, and remanent magnetization, M_r.

***w*, wt% Ni**	**σ, S cm^{-1}**	**M_s, emu g^{-1}**	**M_r, emu g^{-1}**
0	1.87	0.20	0.001
7.2	1.96×10^{-2}	1.65	0.008
19.9	4.33×10^{-3}	8.45	0.033
29.4	8.33×10^{-3}	14.0	0.063
40.2	3.39×10^{-2}	19.5	0.130
53.7	1.29×10^{-2}	27.3	0.137

58.8	3.62×10^{-2}	34.5	0.268
100	≈1000[a]	55.4	2.26

[a] Could not be compressed to a compact pellet. Measured as a powder upon 10 MPa pressure.

The resistivity of composite powders was measured as a function of pressure. This parameter was found to decrease linearly in the double-logarithmic presentation (Fig. 8). It should be stressed that resistivity, and not a resistance, is determined in the present experimental setup. The resistivity decrease (i.e. the conductivity increase) by one up to two orders magnitude can be achieved by the compression.

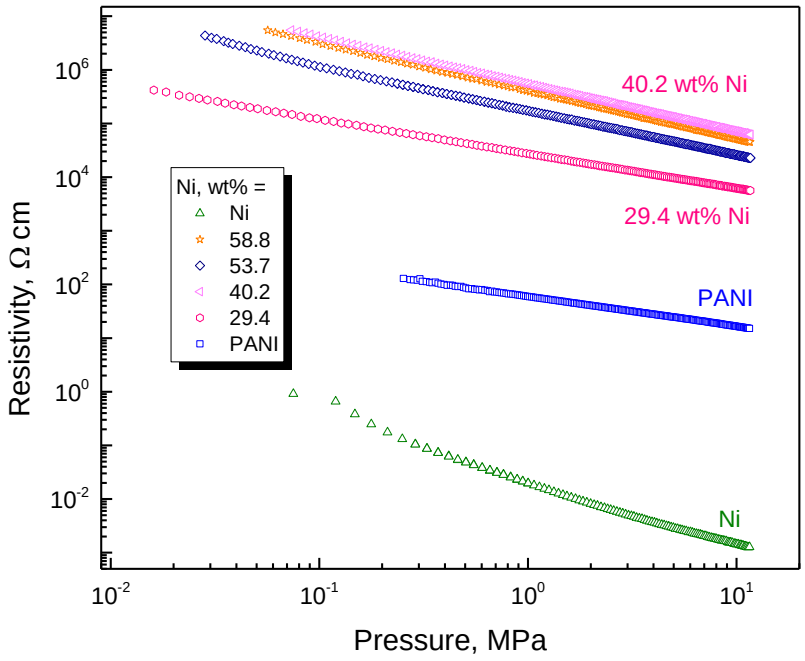

Fig. 8. The dependence of the resistivity of polyaniline/nickel powders and their components (PANI and Ni) on applied pressure.

3.6. Magnetic properties

Magnetisation curves of polyaniline/nickel hybrids (Fig. 9) demonstrate that the saturation magnetisation M_s is reached in fields of 5000 Oe. The original nickel particles are characterised by high value of saturation and remanent magnetization, 55.4 emu g^{-1} and 2.26 emu g^{-1}, respectively (Table 3). Polyaniline alone displayed only a marginal saturation magnetization, 0.20 emu g^{-1}. The magnetic parameters steadily increased with the increasing content of nickel as expected.

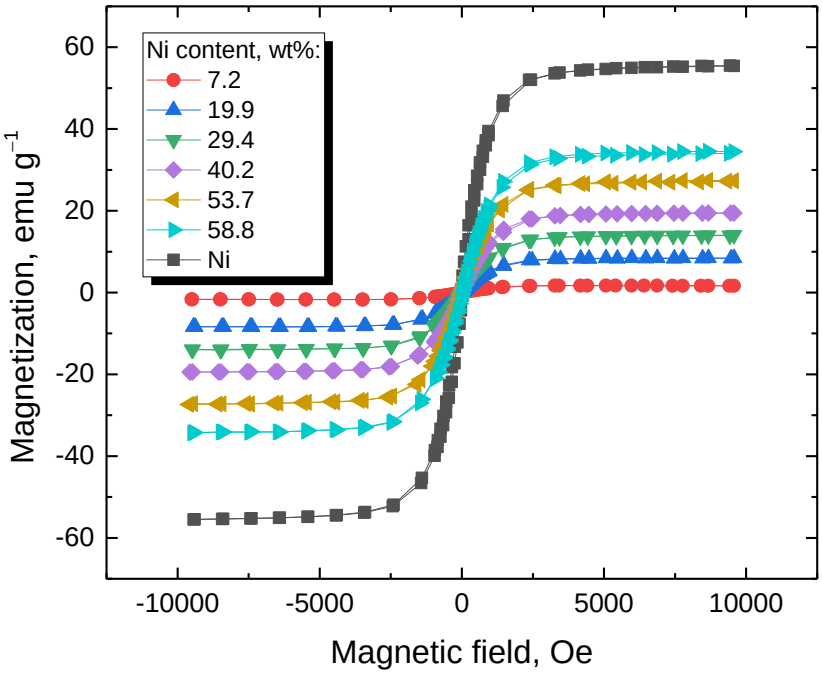

Fig. 9. The dependence of magnetization of polyaniline/nickel composites on applied magnetic field.

3.7. Polyaniline/nickel/polyurethane composites

For practical applications, illustrated below by the electromagnetic interference shielding, the polyaniline/nickel hybrids have to be converted to materials with suitable mechanical properties (Table 4). For that reason, the hybrid powders were dispersed in a matrix of thermoplastic polyurethane (TPU).

Table 4. Mechanical properties of composites at 60 wt% filler content in dependence on nickel content in the polyaniline/nickel filler, *w*: Young modulus, *E*, elongation at break, ε, and ultimate tensile strength, σ_m.

***w*, wt% Ni**	***E* , MPa**	**ε, %**	**σ_m, MPa**
TPU[a]	*23*	*703*	*37*
0	130	1.7	2.4
19.9	306	5.1	10
58.8	140	14	7.1
100	39	327	12

[a] Polyurethane matrix without any filler.

The matrix itself exhibits a typical elastomeric behaviour with a relatively low Young modulus and tensile strength but excellent elongation in the order of hundreds of percent (Table 4). The addition of polyaniline or polyaniline/nickel filler leads to stiffening of polyurethane while lowering elongation and maximum tensile strength. This is the result of the intimate interaction between the both organic components, TPU matrix and polyaniline [30]. The limited interfacial interaction between neat nickel particles and matrix brings back the elastomeric behaviour of composite, however reduced in the comparison with TPU because the nickel particles act as defects stimulating the break at lower tensile strengths.

3.8. Electromagnetic interference shielding

The materials for electromagnetic interference shielding are objects of extensive research [31–37]. The composites based on conducting polyaniline contain as a rule an inorganic component, which is conducting and/or magnetic and a supporting material that provides the mechanical or other materials properties. Due to the wide selections of the components, their distribution, various compositions, and a variety of morphological forms, the performance is difficult to compare.

Conducting polymers have often been used for the surface modification of various supports in order to achieve shielding efficiency in GHz region [31, 32]. They promote especially the radiation reflection contribution while the absorption of radiation is low [33]. The absorption contribution can be increased by the addition of a ferromagnetic component. Here, nickel was tested in the combination of polyaniline for this purpose.

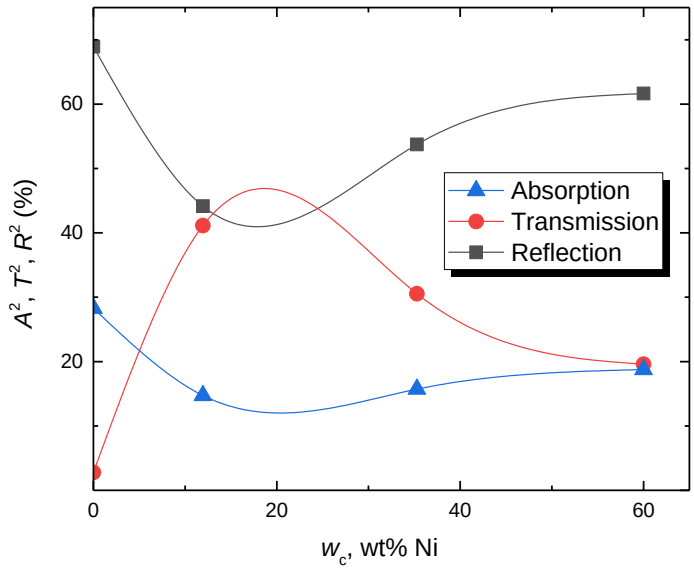

Fig. 10. Absorption, transmission, and reflection contribution to the electromagnetic interference shielding at 9 GHz in dependence on nickel content in the composite with TPU matrix at 60 wt% polyaniline/nickel fillers, $w_c = 0.6\ w$.

Figure 10 shows the dependence of absorption, transmission and reflection contributions on nickel content in composite materials at the same 60 wt% filler content. This means that as the nickel content increases, the content of polyaniline increases accordingly. The composite based exclusively on polyaniline had low transmission, ≈3 %. This is also due to higher volume fraction of polyaniline because of its much lower density compared to nickel. The composite containing neat nickel reflects and absorbs about 60 and 20 % of radiation, respectively and about 20 % of the energy of electromagnetic wave is transmitted. It might be expected that the combination of polyaniline and nickel would leads to properties similar to these fillers, however, their transmission reached even ≈40 % (Fig. 10). This trend copies the conductivity pattern of polyaniline/nickel hybrids that have the conductivity lower than any of their constituents (Table 2, Fig. 2). This is caused by the presence of partly reduced polyaniline with excess of non-conducting quinonedimine units (Fig. 2), which does not contribute to shielding. Hence the reflection and absorption of the composites are mostly given by the nickel content. But still, less than 50 % energy of the electromagnetic wave was transmitted through such a composite at 2 mm sample thickness.

4. Conclusions

Polyaniline/nickel composites were prepared by the oxidation of aniline hydrochloride with ammonium peroxydisulfate in aqueous medium containing nickel microparticles. As the oxidation proceeded, sulfuric acid had been generated as a by-product. In contrast to hydrochloric acid, which does not dissolve nickel, sulfuric acid does. This resulted in the partial dissolution of nickel and the consequent decrease in yield and nickel content in the composites. Hydrogen gas generated during the dissolution caused a partial hydrogenation of polyaniline catalysed by nickel, and reduced the degree of protonation in polyaniline. This led to the decrease in the conductivity of composites to 10^{-3}–10^{-2} S cm^{-1}, i.e. below the conductivity of polyaniline alone, 1.87 S cm^{-1}, and nickel powder ≈1000 S cm^{-1}. This is also due to the fact that the individual nickel microparticles are separated in polyaniline with reduced degree of protonation. Polyaniline/nickel fillers dispersed in the matrix of thermoplastic polyurethane were further tested for shielding efficiency at 9 GHz. The composites were able to absorb and reflect more than 50 % of the energy of the incident electromagnetic wave at 60 wt% loading

and 2 mm sample thickness. It should be noted, however, that those based on individual components were even more efficient, thus reducing the transmission below 20 % and 3 % for nickel and polyaniline dispersed in polyurethane matrix, respectively.

CRediT authorship contribution statement

Marek Jurča: Data acquisition; Data curation. **Jarmila Vilčáková:** Investigation; Supervision; Funding acquisition. **Natalia E. Kazantseva:** Data acquisition; Data curation. **Jan Prokeš:** Formal analysis; Methodology. **Miroslava Trchová:** Data acquisition; Data curation. **Jaroslav Stejskal:** Supervision; Writing – Original draft.

Declaration of competing interest

The authors declare no competing financial interests.

Acknowledgments

The support of the Ministry of Education, Youth and Sports of the Czech Republic (DKRVO RP/CPC/2020/005), Technology Agency of the Czech Republic (Epsilon TH71020006 and Theta TK03030157), and the Czech Science Foundation (22-25734S) is gratefully acknowledged.

References

[1] Stejskal J, Trchová M, Bober P, Humpolíček P, Kašpárková V, Sapurina I, Shishov MA, Varga, M. Conducting Polymers: Polyaniline. In: Encyclopedia of Polymer Science and Technology, Wiley Online Library, pp. 1–44; Wiley, 2015. doi: 10.1002/0471440264.pst640.

[2] Dong XL, Zhang XF, Huang H, Zuo F. Enhanced microwave absorption in Ni/polyaniline nanocomposites by dual dielectric relaxation. Appl Phys Lett 2008;92:013127. doi: 10.1063/1.2830995

[3] Wang JH, Or SW, Tan J. Enhanced microwave electromagnetic properties of core/shell-structured Ni/SiO_2/polyaniline hexagonal nanoflake composites with preferred magnetization and polarization orientations. Mater Design 2018;153:190–202. doi: 10.1016/j.matdes.2018.05.007

[4] Moon IJ, Kim MW, Choi HJ, Kim N, You CY. Fabrication of dopamine grafted polyaniline/carbonyl iron core-shell typed microspheres and their magnetorheology. Colloid Surf A 2016;500:137–145. doi: 10.1016/j.colsurfa.2016.04.037

[5] Tian XL, He K, Wang BX, Yu SS, Hao CC, Chen KZ, Lei QQ. Flower-like Fe_2O_3/polyaniline core/shell nanocomposite and its electrorheological properties. Colloid Surf A 2016;498:185–193. doi: 10.1016/j.colsurfa.2016.03.054

[6] Chowdhury AN, Islam MS, Azam MS. Polyaniline matrix containing nickel ferromagnet. J Appl Polym Sci 2005;103:321–327. doi: 10.1002/app.23958

[7] Chen XL. Wang XW. Li LD. Qi SH. Preparation and microwave absorbing properties of nickel-coated carbon fiber with polyaniline via in situ polymerization. J Mater Sci Mater Electron 2016;27:5607–5612. doi: 10.1007/s10854-016-4466-9

[8] Zhao B, Dong JS, Zhang R, Liang LY, Fan BB, Bai ZY, Shao G, Park CH. Recent advances on the electromagnetic wave absorption properties of Ni base materials. Eng Sci 2018;3:5–40. doi: 10.30919/es8d735

[9] Gao H, Wang CH, Yang ZJ, Zhang Y. 3D porous nickel metal foam/polyaniline heterostructure with excellent electromagnetic interference shielding capability and superior absorption based on pre-constructed macroscopic conductive framework. Compos Sci Technol 2021;213:108896. doi: 10.1016/j.compscitech.2021.108896

[10] Heinig NF, Kharbanda N, Pynenburg MR, Zhou XJ, Schultz GA, Leung KT. The growth of nickel nanoparticles on conductive polymer composite electrodes. Mater Lett 2008;62:2285–2288. doi: 10.1016/j.matlet.2007.11.094

[11] Corte DAD, Torres C, Correa P, dos Santos P, Rieder ES, Malfatti CD. The hydrogen evolution reaction on nickel–polyaniline composite electrodes. Int J Hydrogen Energy 2012;37:3025–3032. doi: 10.1016/j.ijthydene.2011.11.037

[12] Zhang TT, Zhang JL, Zou DC, Cheng F, Su RX. A promising Pd/polyaniline/foam nickel composite electrode for effectively electrocatalytic degradation of methyl orange in wastewater. Desalin Water Treatment 2020;189:386–394. doi: 10.5004/dwt.2020.25566

[13] Wang MY, Tremblay PL, Zhang T. Optimizing the electrical conductivity of polyacrylonitrile/polyaniline with nickel nanoparticles for the enhanced electrostimulation of Schwann cells proliferation. Bioelectrochemistry 2021;140:107770. doi: 10.1016/j.bioelechem.2021.107750.

[14] Damian A, Omanovic S. Ni and Ni-Mo hydrogen evolution electrocatalysts electrodeposited in polyaniline matrix. J Power Sources 2006;158:464–476 (2006). doi: 10.1016/j.jpowsour.2005.09.007

[15] Shah SS, Das HT, Barai HR, Aziz MA. Boosting the electrochemical performance of polyaniline by one-step electrochemical deposition on nickel foam for high-performance asymmetric supercapacitor. Polymers 2022;14:270. doi: 10.3390/polym14020270

[16] Stejskal J. Interaction of conducting polymers, polyaniline and polypyrrole, with organic dyes: polymer morphology control, dye adsorption and photocatalytic decomposition. Chem Pap 2020;74:1–54. doi: 10.1007/s11696-019-00982-9

[17] Bhaumik M, Choi HJ, McCrindle RI, Maity A. Composite nanofibers prepared from metallic iron nano particles and polyaniline: high performance for water treatment applications. J Colloid Interface Sci 2014;425:75–82. doi: 10.1016/j.jcis.201403.031

[18] Guo WL, Hao FF, Yue XX, Liu ZH, Zhang QY, Li XH, Wei J. Rhodamine B removal using polyaniline-supported zero-valent iron powder in the presence of dissolved oxygen. Environ Prog Sustain Energy 2016;35:48–55. doi: 10.1002/ep.12185

[19] Ayad MM, Amer WA, Kotp MG. Magnetic polyaniline-chitosan composites decorated with palladium nanoparticles for enhanced catalytic reduction of 4-nitrophenol. Mol Catal 2017;439:72–80. doi: 10.1016/j.mcat.2017.06.023

[20] Shahriman MS, Zain NNM, Mohamad S, Manan NSA, Yaman SM, Asman S, Raoov M. Polyaniline modified magnetic nanoparticles coated with dicationic ionic liquid for effective removal of rhodamine B (RB) from aqueous solution. RSC Adv 2018; 8:33180–33192. doi: 10.1039/c8ra06687f

[21] Ahmad N, Sultana S, Kumar G, Zuhaib M, Sabir S. Polyaniline base hybrid bionanocomposites with enhanced visible light photocatalytic activity and antifungal activity. J Environ Chem Eng 2019;7:102804. doi: 10.1016/j.jece.2018.11.048

[22] Muhammad A, Shah AUA, Bilal S, Rahman G, Basic Blue dye adsorption from water using polyaniline/magnetite (Fe_3O_4) composites: kinetic and thermodynamic aspects. Materials 2019;12:1764. doi:10.3390/ma12111764

[23] Bhaumik M, Maity A, Brink HG. Metallic nickel nanoparticles supported polyaniline nanotubes as heterogeneous Fenton-like catalyst for the degradation of brilliant green dye in aqueous solution. J Colloid Interface Sci 2022;611:408–420. doi: 10.1016/j.jcis.2021.11.181

[24] Bhaumik M, Majty A, Brink HG. Zero valent nickel nanoparticles decorated polyaniline nanotubes for the efficient removal of Pb(II) from aqueous solution: synthesis, characterization and mechanism investigation. Chem Eng J 2021;417:127910. doi: 10.1016/j.cej.2020.127910

[25] Qu YP, Wang ZY, Xie PT, Wang ZX, Fan RH. Ultraweakly and fine-tunable negative permittivity of polyaniline/nickel metacomposites with high-frequency diamagnetic response. Compos Sci Technol 2022;217:109092. doi: 10.1016/j.compscitech.2021.109092

[26] Xu P. Han XJ, Wang C, Ahou DH, Lv ZS, Wen AH, Wang XH, Zhang B. Synthesis of electromagnetic functionalized nickel/polypyrrole core shell composites. J Phys Chem B 2018;112:10443–10449. doi: 10.1021/jp804327k

[27] Prokeš J, Stejskal J. Polyaniline prepared in the presence of various acids 2. Thermal stability of conductivity, Polym Degrad Stabil 2004;86:187–195. doi: 10.1016/j.polymdegstab.2004.04.012

[28] Stejskal J, Gilbert RG. Polyaniline. Preparation of a conducting polymer (IUPAC technical report). Pure Appl Chem 2002;74:857–867. doi:10.1351/pac200274050857

[29] Itagaki M, Nakazawa H, Watanabe K,Noda K. Study of dissolution mechanisms of nickel in sulfuric acid solution by electrochemical quartz crystal microbalance. Corros Sci 1997;39:901–911. doi: 10.1016/S0010-938X(97)81157-2

[30] Teixeira J, Horta-Romarís L, Abad MJ, Costa P, Lanceros-Méndez S. Piezoresistive response of extruded polyaniline/(styrene-butadiene-styrene) polymer blends for force and deformation sensors. Mater Des 2018;141:1–8. doi: 10.1016/j.matdes.2017.12.011

[31] Chung DDL. Materials for electromagnetic interference shielding. J Mater Eng Perform 2000;9:350–354. doi: 0.1361/105994900770346042

[32] Wang Y, Du YC, Ping X, Qiang R, Han XJ. Recent advances in conjugated polymer-based microwave absorbing materials. Polymers 2017;9:29. doi: 10.3390/polym9010029

[33] Stejskal J, Sapurina I, Vilčáková J, Jurča M, Trchová M, Kolská Z, Prokeš J, Křivka I. One-pot preparation of conducting melamine/polypyrrole/magnetite ferrosponge. ACS Appl Polym Mater 2021;3:1107–1115. doi: 10.1021/acsapm.0c01331

[34] He ZW, Xie HM, Wu HQ, Chen JH, Ma SY, Duan X, Chen AQ, Kong Z. Recent advances in MXene/polyaniline-based composites for electrochemical devices and electromagnetic interference shielding applications. ACS Omega 2021;6:22468–22477. doi: 10.1021/acsomega.1c02996

[35] Soares BG, Barra GMO, Indrusiak T, Conducting polymeric composites based on intrinsically conducting polymers as electromagnetic interference shielding/microwave absorbing materials - a review. J Compos Sci 2021;5:173. doi: 10.3390/jcs5070173

[36] Zahid M, Anum R, Siddique S, Shakir HF, Rehan ZA. Polyaniline-based nanocomposites for electromagnetic interference shielding applications: a review. J Thermoplast Compos Mater 2021;early access. doi: 10.1177/08927057211022408

[37] Shahapurkar K, Gelaw M, Tirth V, Soudagar MEM, Shahapurkar P, Mujtaba MA, Kiran MC, Ahmed GMS. Comprehensive review on polymer composites as electromagnetic

interference shielding materials. Polym Polym Compos 2022;30:09673911221102127. doi: 10.1177/09673911221102127